

EXPERT
REVIEWS

Properties of targeted preamplification in DNA and cDNA quantification

Expert Rev. Mol. Diagn. 15(8), 1085–1100 (2015)

Daniel Andersson^{‡1},
Nina Akrap^{‡1},
David Svec^{1–3},
Tony E Godfrey⁴,
Mikael Kubista^{2,3},
Göran Landberg¹ and
Anders Ståhlberg*^{1,3}

¹Sahlgrenska Cancer Center,
Department of Pathology, Sahlgrenska
Academy at University of Gothenburg,
Box 425, 40530 Gothenburg, Sweden
²Institute of Biotechnology, Academy of
Sciences of the Czech Republic,
Videnska 1083, Prague 4, 14221,
Czech Republic

³TATAA Biocenter, Odinsgatan 28,
41103 Gothenburg, Sweden

⁴Department of Surgery, Boston
University School of Medicine,
700 Albany St. W408D, Boston,
MA 02118, USA

*Author for correspondence:
Tel.: +46 317 866 735
anders.stahlberg@gu.se

[‡]Authors contributed equally

Objective: Quantification of small molecule numbers often requires preamplification to generate enough copies for accurate downstream enumerations. Here, we studied experimental parameters in targeted preamplification and their effects on downstream quantitative real-time PCR (qPCR). **Methods:** To evaluate different strategies, we monitored the preamplification reaction in real-time using SYBR Green detection chemistry followed by melting curve analysis. Furthermore, individual targets were evaluated by qPCR. **Result:** The preamplification reaction performed best when a large number of primer pairs was included in the primer pool. In addition, preamplification efficiency, reproducibility and specificity were found to depend on the number of template molecules present, primer concentration, annealing time and annealing temperature. The amount of nonspecific PCR products could also be reduced about 1000-fold using bovine serum albumin, glycerol and formamide in the preamplification. **Conclusion:** On the basis of our findings, we provide recommendations how to perform robust and highly accurate targeted preamplification in combination with qPCR or next-generation sequencing.

KEYWORDS: experimental design • multiplex PCR • preamplification • primer-pools • quantitative real-time PCR • single-cell analysis • targeted preamplification

Today, many research studies and clinical assessments are based on DNA and RNA analyses of limited sample sizes, including rare tissues, liquid biopsies, fine-needle aspirates and single cells. Numerous techniques to analyze individual cells are available, and single-cell analysis has become a powerful tool to identify and characterize distinct cell types and cell states, as well as to decipher molecular processes relevant in development and disease [1–4]. Single-cell studies have revealed large cell-to-cell variability, even within seemingly homogenous populations, and we have only started to understand the role and importance of different molecular concentrations in cells and their impact on cellular functions and signaling [5,6]. The analysis of DNA and RNA in a few or single cells with quantitative real-time PCR (qPCR) or next-generation sequencing usually requires that the material is preamplified to a level that is compatible with method

constraints (FIGURE 1A). Preamplification can be either global, targeting all molecules in an unselective manner [7,8], or specific, targeting sequences of interest only [9–13]. The most common strategy for targeted preamplification is based on multiplex PCR using pools of specific primer pairs [14]. The preamplification PCR is performed in a limited number of cycles to avoid competition for reagents among the parallel reactions. To reduce the formation of non-specific PCR products, the applied primer concentration is 10–20 times lower than a standard PCR. To compensate for the lower primer concentration, the annealing time is usually extended up to several minutes. The properties and limitations of targeted preamplification in DNA and cDNA quantification are poorly understood, despite its wide application.

In this work, we studied targeted preamplification in detail. To assess its overall performance, we monitored the preamplification

This is an open-access article distributed under the terms of the CC-BY-NC-ND 3.0 License which permits users to download and share the article for non-commercial purposes, so long as the article is reproduced in the whole without changes, and provided the original source is credited.

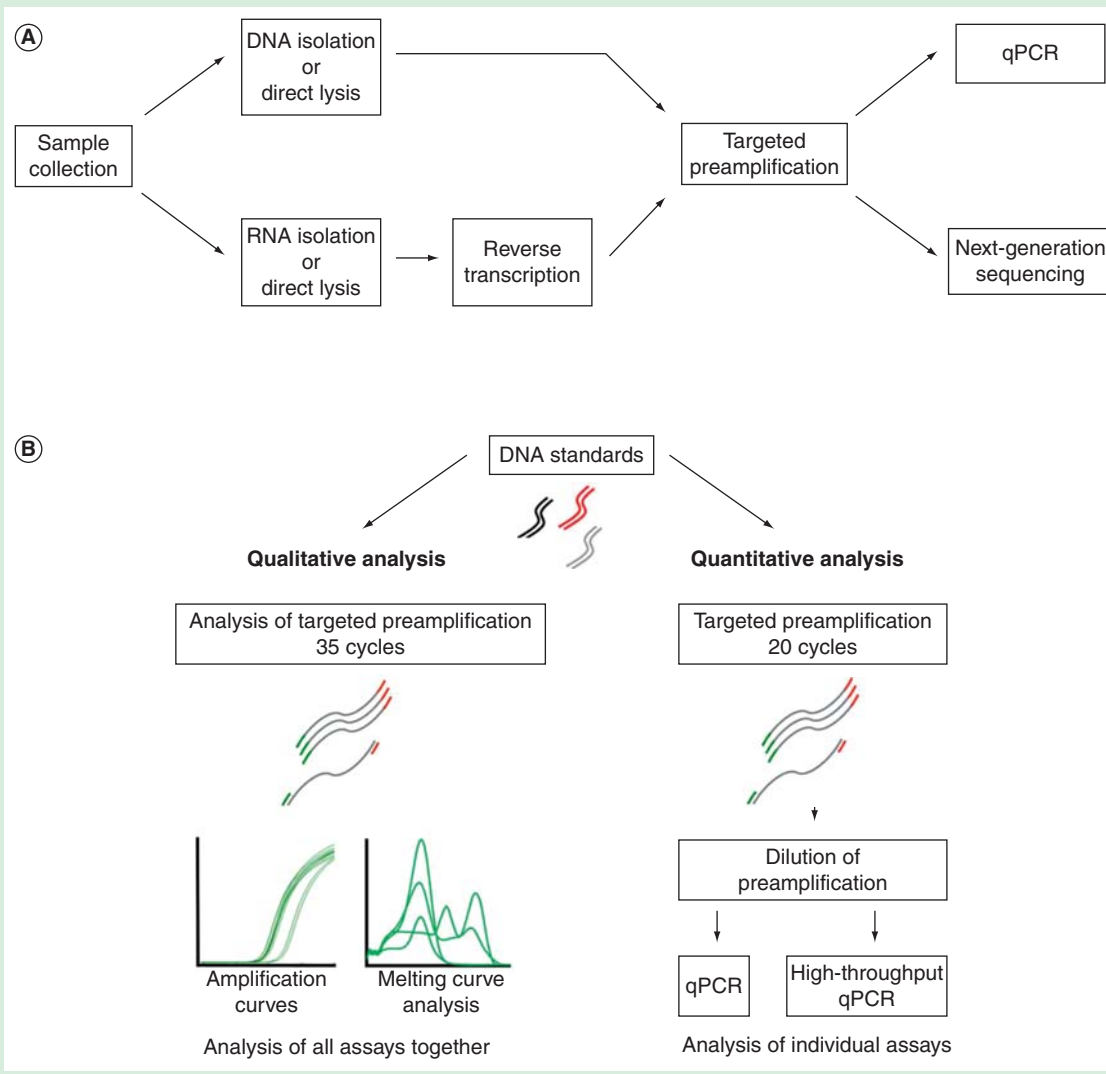


Figure 1. (A) Overview of RNA and DNA analysis using qPCR and next-generation sequencing for small sample sizes. (B) Experimental setup evaluating the properties of targeted preamplification.

reaction in real-time using SYBR Green I detection chemistry followed by melting curve analysis. Furthermore, the formation of specific amplicons was evaluated with standard qPCR (FIGURE 1B). We estimated the impact of assay numbers used, template and primer-pool concentrations, annealing-time and temperature on the reproducibility, specificity and efficiency of targeted preamplification. To minimize the amount of formed nonspecific PCR products, several additives were tested. Altogether, our data allow us to provide general recommendations for accurate targeted DNA and cDNA preamplification.

Methods

Cell culture & single-cell collection

All cell lines were cultured at 37°C and 5% CO₂. The myxoid liposarcoma cell lines MLS1765-92 and DL221 were cultured in RPMI 1640 GlutaMAX medium supplemented with 5% fetal bovine serum, 50 U/ml penicillin and 50 µg/ml

streptomycin (all Life Technologies). MCF-7 cells and experimentally generated cancer-associated fibroblasts [15] were cultured in DMEM medium supplemented with 10% fetal bovine serum, 2 mM L-glutamine and 1% penicillin/streptomycin (all PAA).

For single-cell collection, MCF-7 cultures were washed with 1X PBS, pH 7.4 (Sigma-Aldrich) and enzymatically dissociated with 0.25% Trypsin-EDTA (PAA). Dead cells were removed with the MACS Dead Cell Removal Kit (Miltenyi Biotec) according to the manufacturer's instructions. Cells were resuspended in 1X PBS, pH 7.4, supplemented with 2% bovine serum albumin (Sigma-Aldrich) and kept at 4°C until sorting. Cell aggregates were removed by filtering through a 35 µm cell strainer (BD Biosciences). Individual cells were sorted into 96-well PCR plates (Life Technologies), containing 5 µl 1 µg/µl bovine serum albumin and 2.5% glycerol (Thermo Scientific) in DNase/RNase-free water (Life Technologies)

using a BD FACSAria II (Becton Dickinson) instrument and the FACSDiva software as previously described [16]. Sorted plates were immediately frozen on dry ice and stored at -80°C .

RNA extraction & reverse transcription

Total RNA was extracted from DL221, MLS1765-92 cell lines and experimentally generated cancer-associated fibroblasts using the RNeasy Mini Kit, including DNase treatment (Qiagen). RIN values were determined with the 2100 Bioanalyzer Instrument (Agilent Technologies) and were larger than nine for all RNA samples. Reverse transcription was performed with SuperScript III reverse transcriptase (Life Technologies) [17]. To each sample containing 500–1000 ng total RNA, 0.5 mM dNTPs, 2.5 μM random hexamers and 2.5 μM oligo(dT₁₅) primers (all Sigma-Aldrich) were added to a total volume of 6.5 μl . Samples were incubated at 65°C for 5 min and subsequently cooled on ice. 100 U SuperScript III, 20 U RNaseOUT, 5 mM dithiothreitol, 50 mM Tris-HCl, pH 8.3, 75 mM KCl and 3 mM MgCl₂ (all Life Technologies, final concentrations are shown) were added to a final volume of 10 μl . The following temperature profile was applied: 25°C for 5 min, 50°C for 60 min, 55°C for 15 min and 70°C for 15 min. cDNA was diluted to a concentration corresponding to 1 ng/ μl with nuclease-free water and stored at -20°C .

Single MCF-7 cell cDNA synthesis was performed using TATAA GrandScript cDNA Synthesis Kit (TATAA Biocenter). Briefly, 2 μl 5X TATAA GrandScript RT Reaction Mix, 0.5 μl TATAA GrandScript RT Enzyme and 2.5 μl water were added to a final volume of 10 μl . The following thermal program was used: 22°C for 5 min, 42°C for 30 min and 85°C for 5 min and samples were stored at -20°C .

PCR assays & quantitative real-time PCR

Quantitative PCR was performed in 6 μl reactions utilizing the 2X TATAA SYBR GrandMaster Mix (TATAA Biocenter), 400 nM of each primer (Sigma-Aldrich) and 2 μl template. PCR assays were designed for 96 human transcripts, applying Primer-BLAST [18]. *In silico* oligonucleotide secondary structure prediction was performed with NetPrimer (PREMIER Biosoft International). Detailed primer information is provided in (SUPPLEMENTARY TABLE 1 [supplementary material can be found online at www.informahhealthcare.com/suppl/14737159.2015.1057124]). All assays were target specific, highly sensitive and exhibited a high dynamic range and reproducibility [19]. No additional nonspecific PCR products were formed within 45 cycles of amplification. All assays have been applied for single-cell gene expression profiling on different cell types, including fibroblasts, myxoid liposarcoma and breast cancer cell lines (data not shown) as described [12,20]. To test for specificity all PCR products were subjected to melting curve analysis and were further validated by gel electrophoresis. Quantitative PCR was performed in a CFX384 Touch Real-Time PCR Detection System (Bio-Rad), applying the following thermal protocol: 95°C for 2 min, followed by 40 cycles of amplification (95°C for 5 s, 60°C for 20 s and 70°C for 20 s). Melting curve analysis was performed in the range of 60°C to 95°C , 0.5°C per 5 s

increments. Cycle of quantification (C_q) values were determined by the second derivative maximum method. Preamplification efficiencies were estimated from standard curves with GenEx (MultiD Analyses). All qPCR experiments were conducted in accordance with the Minimum Information for Publication of Quantitative Real-Time PCR Experiments (MIQE) guidelines [21]. Single-cell data were preprocessed as described [22], and absolute quantification of each cDNA species was performed with known DNA standards [20]. Missing single-cell data were assigned a value of 0.5 cDNA molecules to calculate the geometric mean.

Generation of DNA standards

Reverse transcribed RNA from MLS1765-92, DL221 cells and experimentally generated cancer-associated fibroblasts was used as template in qPCR to generate PCR product standards for all experiments in this study. Specific PCR products were purified with the MinElute PCR Purification Kit (Qiagen) and eluted in EB buffer. DNA concentration was quantified with the Qubit dsDNA HS Assay Kit on the Qubit Fluorometer (Life Technologies) and converted to molecules per microliter [23]. Concentrations of all PCR products were adjusted to 5×10^9 molecules per μl and stored at -20°C .

Targeted DNA preamplification

Preamplification was performed under various experimental conditions: a detailed summary of all tested parameters is shown in TABLE 1. Targeted preamplification was performed in 10 μl reactions, or in 20 μl reactions for MCF-7 single-cells, using 2X TATAA SYBR GrandMaster Mix, 40 nM of each primer and 0.1–2.0 μl template. Identical primer pairs were applied for targeted preamplification and downstream qPCR. One hundred purified DNA molecules of each target sequence were used as template if not stated otherwise. The following thermal profile for targeted preamplification was applied on a T100 Thermal Cycler (Bio-Rad): 95°C for 3 min, followed by 20 cycles of amplification (95°C for 20 s, 60°C for 3 min and 72°C for 20 s). After the final extended (10 min) elongation step, the samples were immediately frozen on dry ice, slowly thawed on ice, diluted 1:20 in 10 mM Tris and 1 mM EDTA, pH 8.0 (Life Technologies) and stored at -20°C until analysis. Individual assay performance was analyzed on the CFX384 Touch Real-Time PCR Detection System or on the BioMark high-throughput qPCR platform (Fluidigm).

To monitor the targeted preamplification reaction in real time, we used SYBR Green I detection chemistry in the CFX384 Touch Real-Time PCR Detection System. The following thermal protocol was used: 95°C for 3 min, followed by 35 cycles of amplification (95°C for 20 s, 60°C for 3 min and 72°C for 20 s). Melting curve analysis was performed in the range of 60°C to 95°C , 0.5°C per 5 s increments. C_q values were determined using a threshold.

Preamplification additives

The effects of 18 different PCR additives on the preamplification reaction were evaluated (final tested concentrations are

Table 1. Summary of analyzed parameters for targeted preamplification.

Tested parameter	Final primer concentration (nM)	Number of assays	Annealing time (min)	Annealing temperature (°C)	Template concentration
Template concentration (FIGURE 2)	40	96	3	60	6 × 100 molecules + 90 × 0–10 ⁷ molecules
Template concentration (FIGURE 3)	40	96	3	60	95 × 100 molecules + 1 × 100–10 ⁹ molecules
Number of assays (FIGURE 4)	40	6, 12, 24, 48, 96	0.5, 3, 8	60	96 × 100 molecules
Primer concentration (FIGURE 5)	10, 40, 160, 240	96	0.5, 3, 8	60	96 × 100 molecules
Annealing temperature (FIGURE 6)	40	96	3	55.0, 56.8, 58.8, 61.3, 63.3, 65.3	96 × 100 molecules
PCR Additives (FIGURE 7)	40	96	3	60	96 × 100 molecules

shown): 7-deaza-2'-deoxyguanosine 5'-triphosphate lithium salt (50 and 100 μM; Sigma-Aldrich), ammonium sulfate (10 and 15 mM; Sigma-Aldrich), betaine (0.25 and 0.50 M; Sigma-Aldrich), bovine serum albumin supplied at 20 mg/ml in 10 mM Tris-HCl, 100 mM KCl, 1 mM EDTA and 50% glycerol (1 and 2 μg/μl; Thermo Scientific), D-(+)-trehalose dehydrate (0.15 and 0.30 M; Sigma-Aldrich), dimethyl sulfoxide (1%; Sigma-Aldrich), dithiothreitol (1.5 and 3.0 mM; Life Technologies), formamide (0.5 M; Sigma-Aldrich), gelatin (0.01 and 0.10%; Sigma-Aldrich), glycerol (2.5 and 5.0%; Sigma-Aldrich), IGEPAL CA-630 (0.25 and 0.50%, Sigma-Aldrich), L-carnitine inner salt (0.25 and 0.50 M; Sigma-Aldrich), GenElute-LPA (50 and 100 ng/μl; Sigma-Aldrich), polyinosinic:polycytidylic acid potassium salt (5 and 50 ng/μl; Sigma-Aldrich), tetramethylammonium chloride (30 and 60 mM; Sigma-Aldrich), Triton X-100 (0.2 and 0.4%; Sigma-Aldrich), TWEEN 20 (0.10 and 0.50%, Sigma-Aldrich) and yeast tRNA (50 and 100 ng/μl, Life Technologies).

High-throughput quantitative real-time PCR

High-throughput qPCR was performed on the BioMark system using the 96.96 Dynamic Array Chip for Gene Expression and EvaGreen-based detection. Each 5 μl sample reaction contained 2 μl diluted preamplification product as template, 2.5 μl SsoFast EvaGreen SuperMix (Bio-Rad), 0.25 μl DNA Binding Dye Sample Loading Reagent (Fluidigm), as well as 0.01 μl ROX (Life Technologies, final concentration in the sample mix was 50 nM) and water. The 5 μl assay reaction mix contained 2.5 μl Assay Loading Reagent (Fluidigm) and 2.5 μl of 10 μM mix of reverse and forward primer. Priming and loading of the dynamic array were performed according to the manufacturer's instructions using the IFC controller HX. The temperature profile was thermal mixing at 70°C for 40 min and 60°C for 30 s, followed by hot start activation at 95°C for 60 s and 40 cycles of amplification (96°C for 5 s and 60°C for 20 s). Melting curve analysis was performed

in the range of 60°C to 95°C at 0.5°C per s increments. Amplification data were analyzed with the Fluidigm Real-Time PCR Analysis software, applying the linear derivative baseline subtraction method and a user-defined global threshold to obtain C_q-values. Melting curve analysis was performed on all the samples.

Results

To study targeted preamplification, we used 96 individually optimized qPCR assays (SUPPLEMENTARY TABLE 1). To control and monitor the effect of variable numbers of molecules, we generated DNA standards based on PCR products for each assay. Preamplification efficiencies of all 96 multiplexed assays were evaluated with standard curves, ranging from 5 to 5120 DNA molecules, applying optimal run conditions: 40 nM of each primer, 60°C annealing temperature and 3 min annealing time. The overall preamplification efficiency was 101.4% (± 3.5%, 95% confidence) (SUPPLEMENTARY FIGURE 1). Individual assay efficiencies are provided in SUPPLEMENTARY TABLE 1. Five of the 96 assays failed in the preamplification reaction.

To investigate the preamplification reaction in detail, we analyzed the performance of the total amount of PCR products formed and each individual assay (FIGURE 1B). Individual assays were evaluated with downstream qPCR after 20 cycles of preamplification, while the overall preamplification performance was monitored over 35 cycles in a real-time qPCR instrument using SYBR Green I detection chemistry. Here, we refer to the latter method as analysis of preamplification. The rationale behind running 35 cycles preamplification was to produce sufficient amount of DNA for melting curve analysis, which allowed us to distinguish between specific and nonspecific PCR products. Applying such large number of cycles drives the reaction beyond its exponential phase, which may alter the ratio of specific to nonspecific PCR products. Still, the analysis of preamplification proved to be the most informative tool providing important insights into the reaction mechanism of targeted preamplification.

The optimal number of preamplification cycles depends on the downstream application, here qPCR. In qPCR, the variation across reaction chambers attributable to the Poisson noise leads to substantial uncertainty in the measured cycle of quantification (C_q). Theoretically, applying the Poisson distribution, with an average of 5 molecules per reaction chamber, we calculate 99.3% probability that a reaction chamber will contain at least one molecule. An average of about 35 molecules per reaction chamber is needed to reduce the variation in C_q due to the Poisson effect below the variation observed for typical qPCR [11,14]. Following preamplification, samples are diluted to inactivate the enzymatic activity still present in the reaction tube and because of the sample loading architecture of high-throughput qPCR platforms. Taking the dilution into account and considering the effect of Poisson noise, we can calculate the number of preamplification cycles required to produce sufficient amount of amplicons for reliable detection and reproducible quantification of the targets in downstream qPCR analysis. SUPPLEMENTARY FIGURE 2 shows that when starting with a sample containing five target molecules, 19 preamplification cycles are required to generate an average of five molecules per reaction chamber in the BioMark high-throughput qPCR platform assuming a preamplification efficiency of 80%. In this study, our optimized assays displayed a preamplification efficiency of approximately 100%, which results in an average of 36 molecules per reaction chamber (SUPPLEMENTARY FIGURE 2).

Dependence on target molecule numbers

To assess the dynamic range of preamplification, we performed two experiments (TABLE 1). In the first experiment, the initial number of target molecules for six of the assays was 100 each per reaction, while the initial number of target molecules for each of the remaining 90 assays was varied from 0 to 10⁷ per reaction (FIGURE 2). In the second experiment, the initial number of target molecules for each of the 95 assays was 100 per reaction, and only for one assay (*IGF2BP3*) the initial amount of target molecules was varied from 100 to 10⁹ per reaction (FIGURE 3).

The preamplification was within dynamic range when 90 targets were initially present at <10⁴ molecules of each per reaction, while the other six target templates remained at a constant concentration of 100 molecules per reaction (FIGURES 2A-2D). The preamplification of all assays was inhibited when >10⁴ molecules of each for the 90 targets were added. However, when the target concentration of only one assay was increased, the preamplification of other assays was not affected (FIGURES 3A-3D). The single assay in this experiment was within dynamic range up to about 10⁵ target molecules per reaction. In conclusion, the preamplification dynamic range of an assay was dependent on the amount of its target molecules and on the total number of target molecules for all the preamplification assays.

Dependence on assay numbers

To assess the effect of different assay numbers in the preamplification reaction, we amplified 6, 12, 24, 48 and 96 pooled assays (TABLE 1) and evaluated the amount of specific and

nonspecific PCR products (FIGURE 4). The total amount of primers increased with increasing assay number, but the primer concentration of each primer was maintained at 40 nM. Analysis of preamplification in FIGURES 4A-4E shows that the total yield increased with increasing assay numbers. The nontemplate controls, with water replacing target molecules, displayed that also the amount of nonspecific PCR product increased with assay number. The most dramatic effect, ~1000 fold (~10 cycles) increase in the amount of nonspecific PCR product formed, was observed when increasing the number of pooled assays from 24 to 48. The amplification curves for the template-containing samples exhibited similar C_q-values as the nontemplate controls when multiplexing 48 or 96 assays, suggesting that specific and nonspecific PCR products were formed at comparable rates. Similar results were obtained with shorter (0.5 min) and longer (8 min) annealing times (SUPPLEMENTARY FIGURES 3 & 4).

The yields of individual assays in downstream qPCR analysis increased with increasing assays in the primer-pool up to the maximum number of 96 assays tested (FIGURES 4F & 4G). In line with these data, the preamplification reproducibility also improved with increasing assay number (FIGURES 4F & 4G). In conclusion, individual assays performed best in the preamplification when high numbers of assays were multiplexed.

Dependence on primer concentration & annealing time

Next, we tested the effect of variable primer concentrations (10, 40, 160, 240 nM, final concentration of each primer) and different annealing times (0.5, 3 and 8 min) (TABLE 1) simultaneously, due to their close inter-relationship in preamplification (FIGURES 5 & SUPPLEMENTARY FIGURE 5). Analysis of preamplification showed that the yields of specific and nonspecific PCR products increased with increasing primer concentration and annealing time (FIGURES 5A-5E). The melting curves of the preamplification products obtained with 3 min annealing revealed a shift from specific to nonspecific PCR product formation when primer concentrations were increased from 40 to 160 nM (FIGURE 5B).

The yields of individual assays in downstream qPCR analysis were also dependent on primer concentration and annealing time (FIGURE 5F). Long annealing times (3 and 8 min) were superior than short (0.5 min), and primer concentrations in the range of 40 to 240 nM outperformed 10 nM. However, at a primer concentration of 40 nM, only a small percentage of the negative controls formed nonspecific PCR products, while at primer concentrations ≥160 nM almost all negative controls did. The preamplification reproducibility was highest at primer concentrations ≥40 nM and annealing times ≥3 min (FIGURE 5G). In conclusion, optimal preamplification was obtained using 40 nM of each primer and 3 min or longer annealing time.

Dependence on annealing temperature

All primers in this study were designed to anneal to their target sequence at 60°C. We evaluated preamplification performance at annealing times ranging from 55.0°C to 65.3°C (TABLE 1 & FIGURE 6). Analysis of preamplification revealed that higher annealing temperature decreased the yields of reactions containing

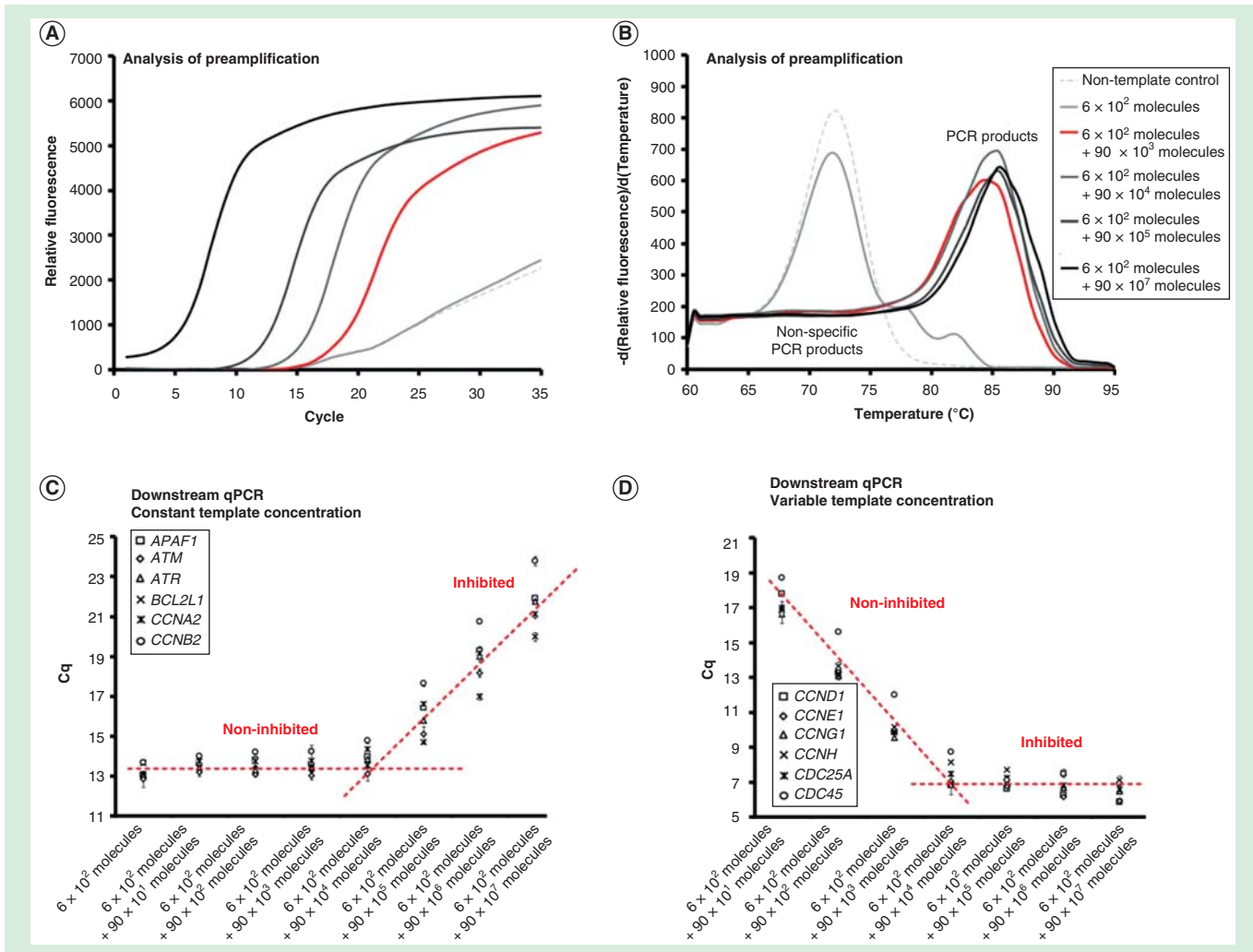


Figure 2. Dynamic range of preamplification – the effect of total template concentration. The preamplification dynamic range with six targets at a constant initial concentration, while increasing the amounts of the other 90 targets. Analysis of preamplification: **(A)** preamplification response curves and corresponding **(B)** melting curves at six selected conditions. **(C)** Average Cq ± SD (n = 3) of the six assays kept at a constant initial template concentration of 100 molecules each per reaction. The linear fit is to guide the eye only. **(D)** Average Cq ± SD (n = 3) of six randomly selected assays from the preamplification with an initial template concentration of 0 to 10⁷ molecules each. The linear fit is to guide the eye only.

template and nontemplate controls (FIGURES 6A-6E). A gradual shift from nonspecific toward specific PCR product formation was observed with increasing annealing temperature (FIGURE 6B). However, even at the highest tested annealing temperature (65.3°C), the relative amount of nonspecific PCR products compared with specific PCR products was maintained.

For downstream qPCR analysis of individual assays, optimal yield was observed at an annealing temperature below 61.3°C, while nonspecific PCR product formation decreased below 2% when the annealing temperature was 58.8°C or higher (FIGURE 6F). Highest reproducibility was obtained using low annealing temperatures (FIGURE 6G). In conclusion, highest yield, specificity and reproducibility in preamplification were obtained at annealing temperatures between 58.8°C and 61.3°C, using assays designed to anneal at 60°C.

Effect of additives on the formation of nonspecific PCR products

Analysis of preamplification revealed large amounts of nonspecific PCR products being formed under most conditions tested (FIGURES 2-6). Therefore, we evaluated the effects of 18 different additives (TABLES 1 & 2) in 35 reaction conditions (FIGURE 7A-7C). We found that 1 and 2 µg/µl bovine serum albumin supplied with 2.5 and 5.0% glycerol, respectively, 5% glycerol, 0.5 M formamide and 0.5 M L-carnitine reduced the formation of nonspecific PCR products by 10 cycles (~1000-fold) compared with preamplification without additives (FIGURE 7C). As an example, FIGURE 7A & 7B shows preamplification and melting curves generated in the presence of 1 µg/µl bovine serum albumin supplemented with 2.5% glycerol relative to water controls.

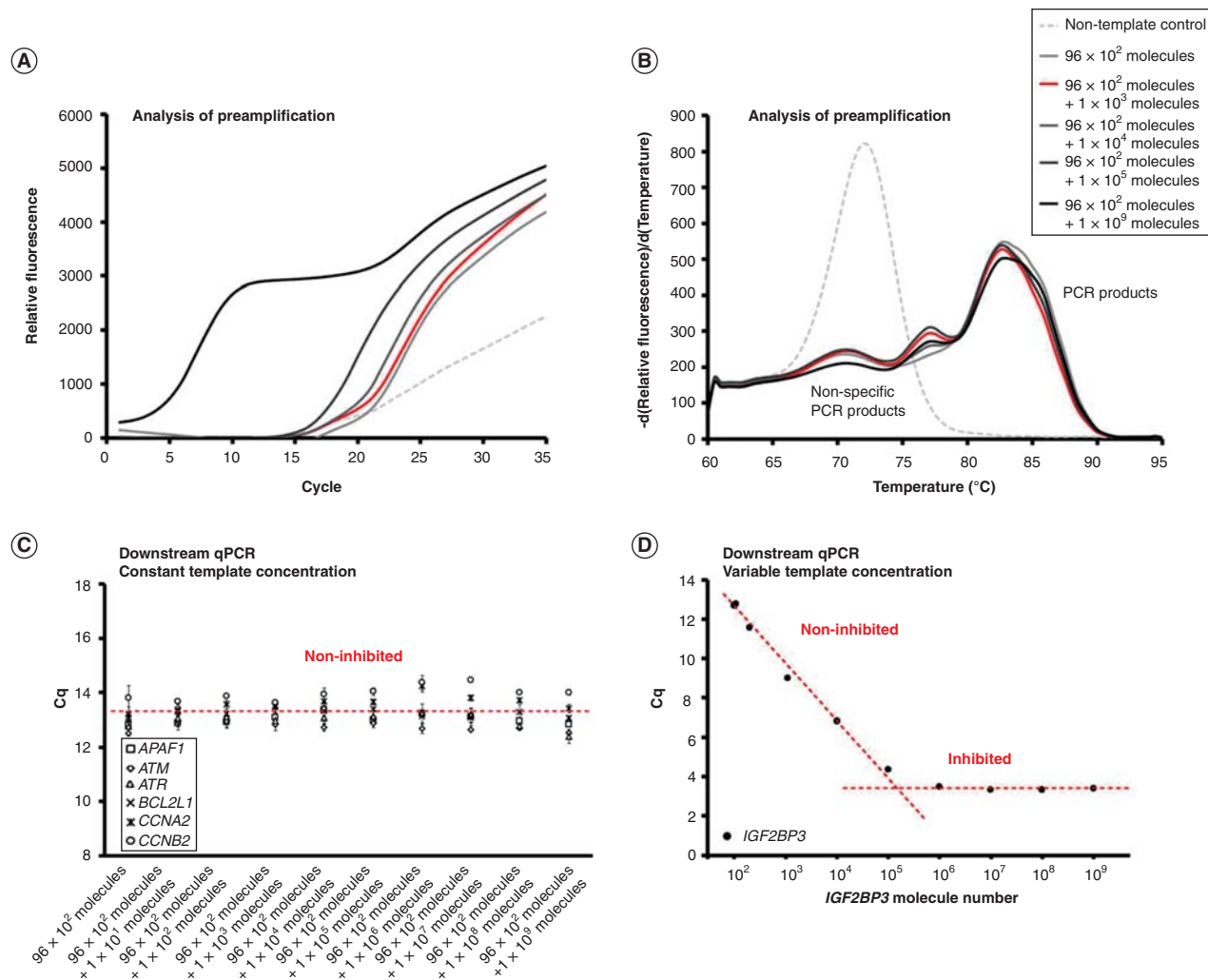


Figure 3. Dynamic range of preamplification – the effect of one target. The preamplification dynamic range of one assay at variable initial target concentration measured in the background of 95 assays with constant target concentrations. Analysis of preamplification: **(A)** preamplification response curves and corresponding **(B)** melting curves at six selected conditions. **(C)** Average Cq \pm SD ($n = 3$) of six randomly selected assays from the preamplification used at a constant initial concentration of 100 molecules each per reaction. The linear fit is to guide the eye only. **(D)** Average Cq \pm SD ($n = 3$) of the single assay included in the preamplification with an initial template concentration of 10^2 to 10^9 molecules. The linear fit is to guide the eye only.

To further assess the function of additives, we performed 20 cycles of targeted preamplification with nine selected additives, followed by downstream qPCR analysis of the 96 individual assays (FIGURE 7D). Here, preamplification without additives was comparable with preamplification with additives in terms of yield and specificity. Some conditions, especially 0.5 M L-carnitine, not only generated lower amount of nonspecific preamplification products but also decreased yields of specific products. In conclusion, the use of 1 $\mu\text{g}/\mu\text{l}$ bovine serum albumin supplemented with 2.5% glycerol and 0.5 M formamide reduced the amount of nonspecific products formed during preamplification, while maintaining high yield and specificity of each specific qPCR.

Single-cell gene expression profiling using targeted preamplification

Single-cell gene expression profiling usually requires targeted preamplification when more than ten genes are analyzed in downstream qPCR analysis [24]. To demonstrate the use of targeted preamplification in single-cell analysis, we profiled 30 individual MCF-7 cells. Single MCF-7 cells were collected with fluorescence-activated cell sorting, lysed and all RNA were reverse transcribed. Twenty percent of each cDNA sample was used for analysis of preamplification (FIGURE 8A & 8B) and another 20% was used for 20 cycles of targeted preamplification followed by downstream qPCR analysis (FIGURE 8C). Targeted preamplification for all single-cell analysis was performed with 1 $\mu\text{g}/\mu\text{l}$

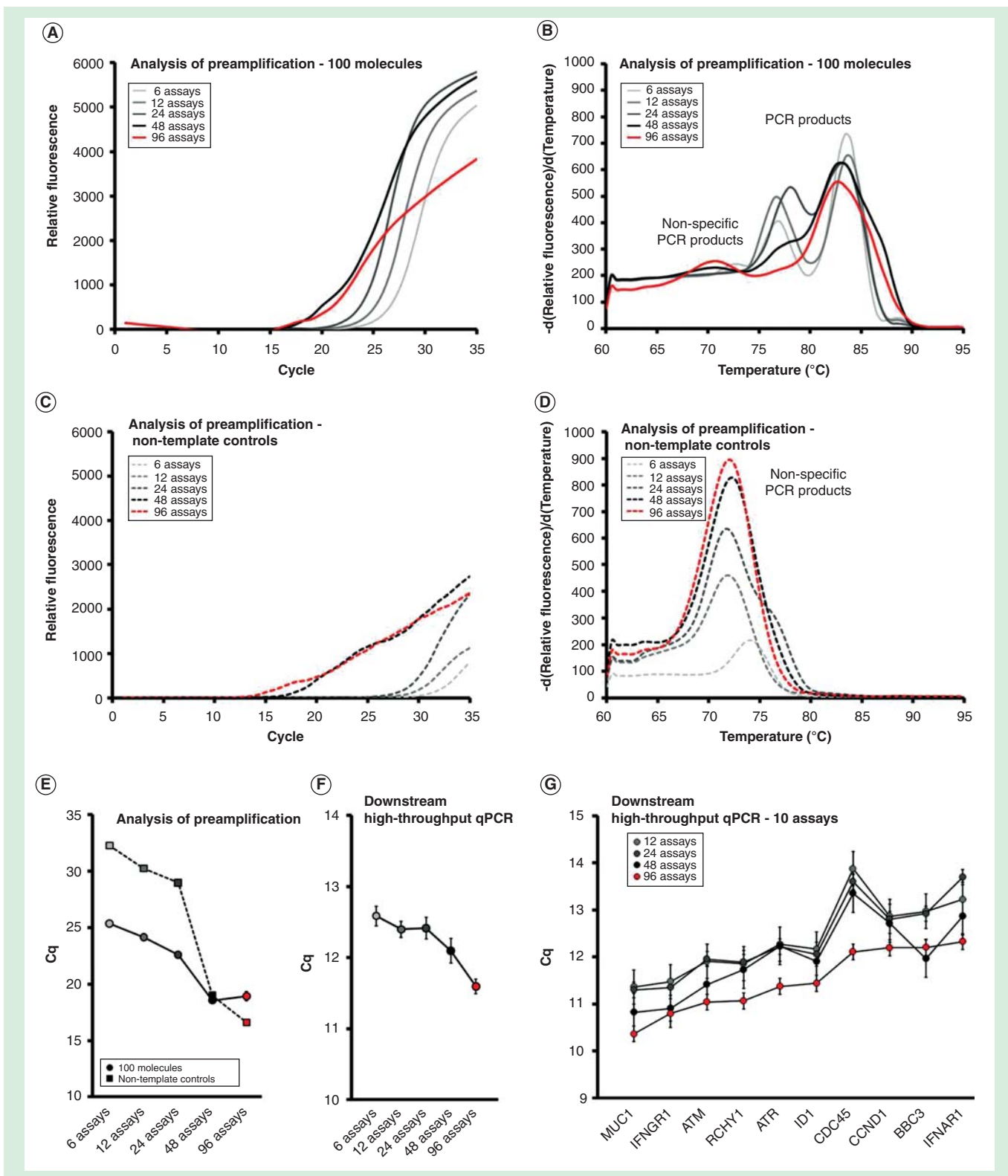


Figure 4. Assay number dependence. The preamplification yield of specific and nonspecific PCR products formed when using 6, 12, 24, 48 and 96 pooled assays. Analysis of preamplification: preamplification response curves and corresponding melting curves for **(A, B)** positive samples and **(C, D)** negative controls. Positive samples contained 100 initial molecules of each target. **(E)** Cq-values (average \pm SD) for positive ($n = 3$) and negative samples ($n = 3$) using different number of assays in preamplification. **(F)** High-throughput qPCR data of individual assays. Average Cq \pm SD ($n = 3$) is shown. Data from all preamplified genes were used. **(G)** Average Cq \pm SD ($n = 3$) of 10 assays included in the preamplification with 12, 24, 48 and 96 pooled assays.

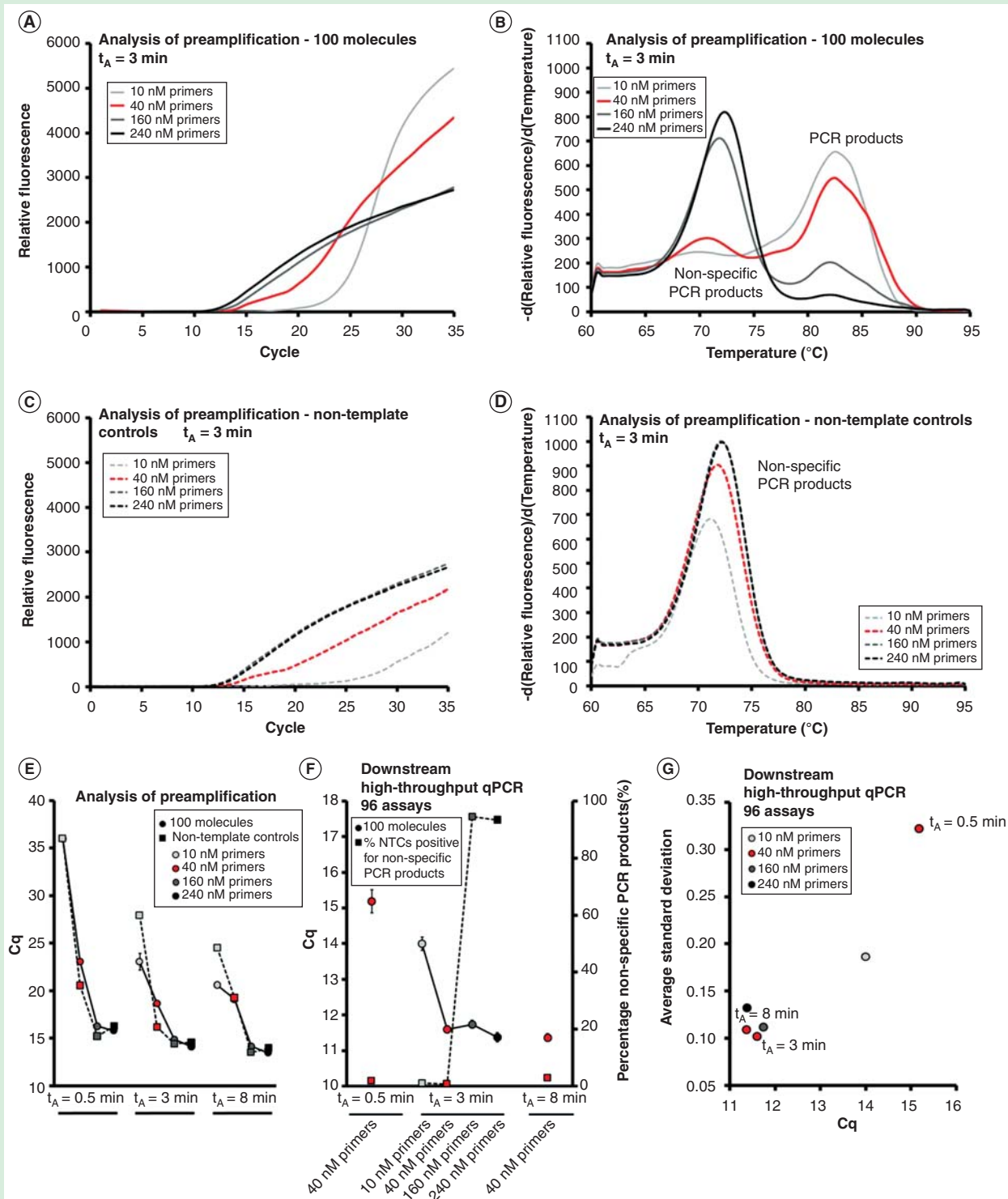


Figure 5. The effect of primer concentration and annealing time. The preamplification yield of specific and nonspecific PCR products formed using different primer concentrations (10, 40, 160 and 240 nM, final individual primer concentrations) and annealing times (0.5, 3 and 8 min). Analysis of preamplification: preamplification response curves and corresponding melting curves for **(A, B)** positive samples and **(C, D)** negative controls. Positive samples contained 100 initial molecules of each target. **(E)** Average $C_q \pm$ SD for positive ($n = 3$) and negative samples ($n = 3$) using different number of assays in preamplification. **(F)** High-throughput qPCR data of individual assays. Average $C_q \pm$ SD ($n = 3$) is shown. The right y-axis indicates the percentage of negative controls positive for nonspecific PCR product formation, calculated from the 91 assays performing accurately in the preamplification ($n_{\text{total}} = 273$, 3 negative qPCR controls per assay). **(G)** Average SD of C_q versus average C_q -value for all individual assays. NTC: Non-template control.

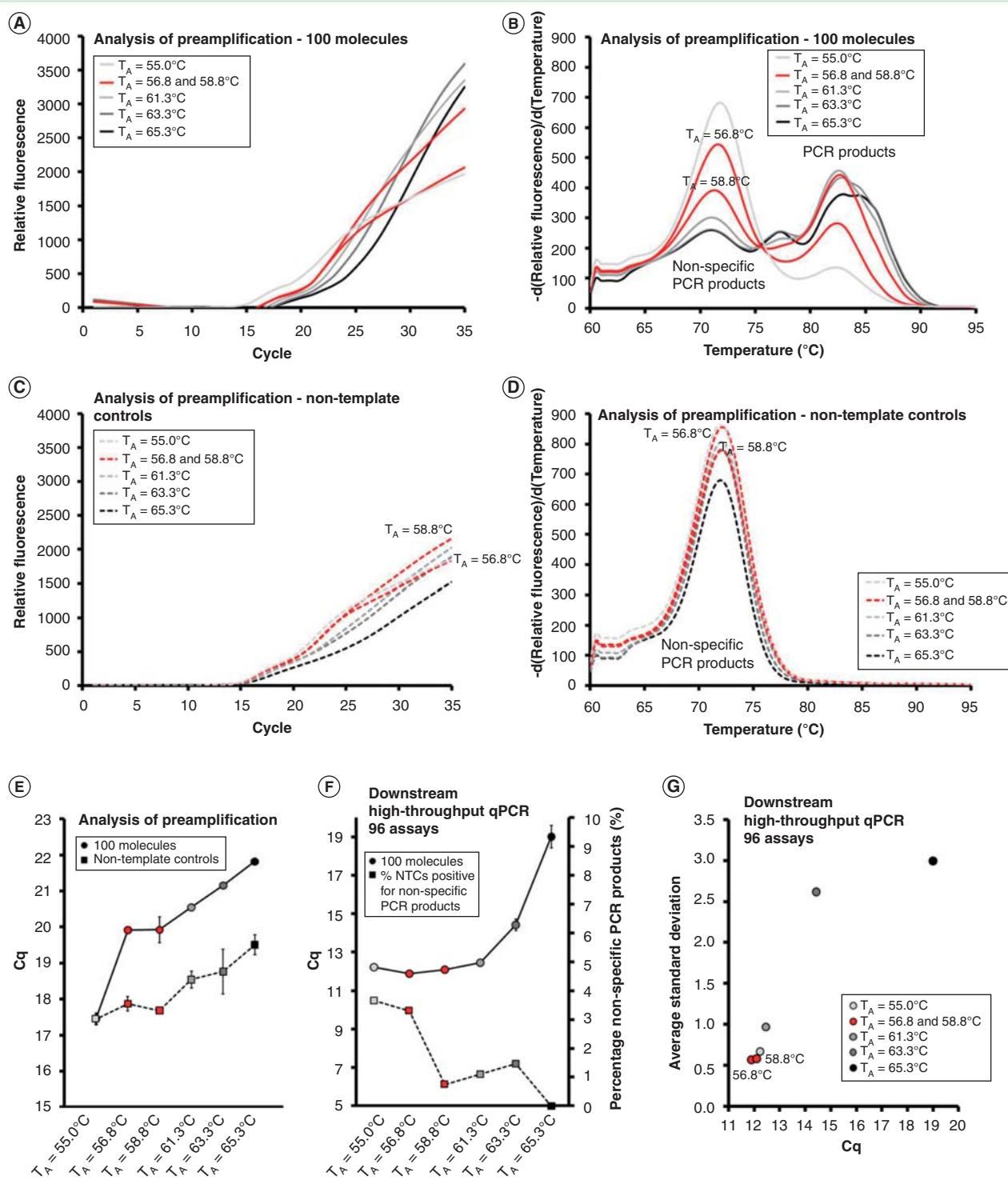


Figure 6. The effect of primer annealing temperature. Preamplification yields of specific and nonspecific PCR products formed as function of the annealing temperature used. Annealing temperatures ranged between 55.0 and 65.3°C. Analysis of preamplification: preamplification curves and corresponding melting curves for **(A, B)** positive samples and **(C, D)** negative controls. Positive samples contained 100 initial molecules of each target. **(E)** Average Cq \pm SD for positive ($n = 3$) and negative samples ($n = 3$) using different annealing temperatures. **(F)** High-throughput qPCR data of individual assays. Average Cq \pm SD ($n = 3$) is shown. The right y-axis indicates the percentage of negative controls positive for nonspecific PCR product formation, calculated from the 91 assays performing accurately in the preamplification ($N_{\text{total}} = 273$, 3 negative qPCR controls per assay). **(G)** Average SD of Cq versus average Cq-value for all individual assays. NTC: Non-template control.

l bovine serum albumin supplemented with 2.5% glycerol using the primer-pool of all 96 assays. FIGURE 8A & 8B indicate that the amounts of specific PCR products generated from all individual cells were low, but detectable.

Downstream qPCR analysis allowed us to estimate the number of cDNA molecules per individual MCF-7 cell using the generated DNA standards (FIGURE 8C). As expected, transcripts showed lognormal features among the individual cells [5]. The transcript variability ranged about two orders of magnitude for most genes. For *RPS10* with highest geometric mean expression (590 cDNA molecules), the cell with lowest expression contained 180 cDNA molecules, while the cell with highest expression contained 1200 cDNA molecules. The number of cDNA molecules for the lowest expressed gene, *SOX9*, with geometric mean expression of 0.80 cDNA molecules ranged between 0 and 24.

Discussion

Today, many clinical applications strive toward the use of noninvasive sampling strategies and small biopsies, including fine needle aspirates and even single cells, to detect and quantify biomarkers. Analysis of liquid biopsies, most commonly blood, is an attractive approach to diagnose and monitor patients over time, since sample collection is standardized and associated with low trauma. However, analysis of biomarkers in liquid biopsies is usually indirect, since target molecules associated with the disease do not originate from the sampled liquid itself. For example, circulating tumor cells and circulating cell-free tumor DNA are derived from the primary tumor or metastases and are therefore only present at low concentrations [25,26]. In addition to enumeration, circulating tumor cells also benefit from being analyzed at the molecular level [27]. Analysis of circulating tumor cells and circulating cell-free tumor DNA holds great promises to add value in clinical decisions, but requires highly sensitive, robust and specific technologies [25–27]. The preferred strategy to quantify multiple DNA or cDNA targets in biological samples of limited size is to first preamplify the material, which theoretically allows for the analysis of any target sequence by downstream qPCR or next-generation sequencing. Optimized preamplification protocols typically show high sensitivity, specificity, efficiency, reproducibility and dynamic range. Targeted preamplification is usually conducted as a multiplex PCR, restricting the amplification to the sequences of interest

Table 2. Summary of analyzed PCR additives applied for targeted cDNA preamplification.

Name	Function	References
7-deaza-2'-deoxyguanosine 5'-triphosphate	Decreases secondary structures caused by GC-rich regions, lowers Tm	[28,29]
Ammonium sulfate	Alternative PCR buffer	[30]
Betaine	Decreases secondary structures caused by GC-rich regions, lowers Tm	[29,31,32]
Bovine serum albumin	Stabilizing agent, carrier, reduce PCR inhibition	[33–35]
D-(+)-trehalose	Decreases secondary structures caused by GC-rich regions, enzyme stabilizer	[36,37]
Dimethyl sulfoxide	Decreases secondary structures caused by GC-rich regions, lowers Tm	[29,32,38]
Dithiothreitol	Enzyme stabilizer	[34]
Formamide	Decreases secondary structures caused by GC-rich regions, lowers Tm	[39]
Gelatin	Enzyme stabilizer, carrier	[40]
GenElute-LPA (linear polyacrylamide)	Carrier	[41]
Glycerol	Lowers Tm, polymerase stabilizer	[42]
IGEPAL CA-630	Surfactant	[5]
L-carnitine	Osmoprotectant	[37]
Polyinosinic–polycytidylic acid	Carrier	[43]
Tetramethylammonium chloride	Increases primer specificity, increases relative Tm of AT-rich regions	[44–46]
Triton X-100	Surfactant	[47]
TWEEN 20	Surfactant	[48]
Yeast tRNA	Carrier	[49]

Tm: Melting temperature.

only [9–13]. Multiplex PCR is a highly complex reaction where the simultaneous amplification of many targets may interfere. Here, we have studied several properties of targeted preamplification and their effects on downstream qPCR analysis.

Robust preamplification requires that the reaction is within its dynamic range. On the one hand, we need to generate sufficient numbers of molecules for reliable detection and accurate quantification. On the other hand, we should not cycle the reaction beyond its exponential phase. Highly abundant RNAs, such as 18S, are commonly targeted in gene expression profiling, but their inclusion in preamplification is usually not recommended. However, here we demonstrate that the presence of one target in high concentration does not necessarily affect the quantification of other targets if the primer concentration becomes the limiting factor. For single-cell experiments analyzed on the high-throughput BioMark platform preamplification is usually

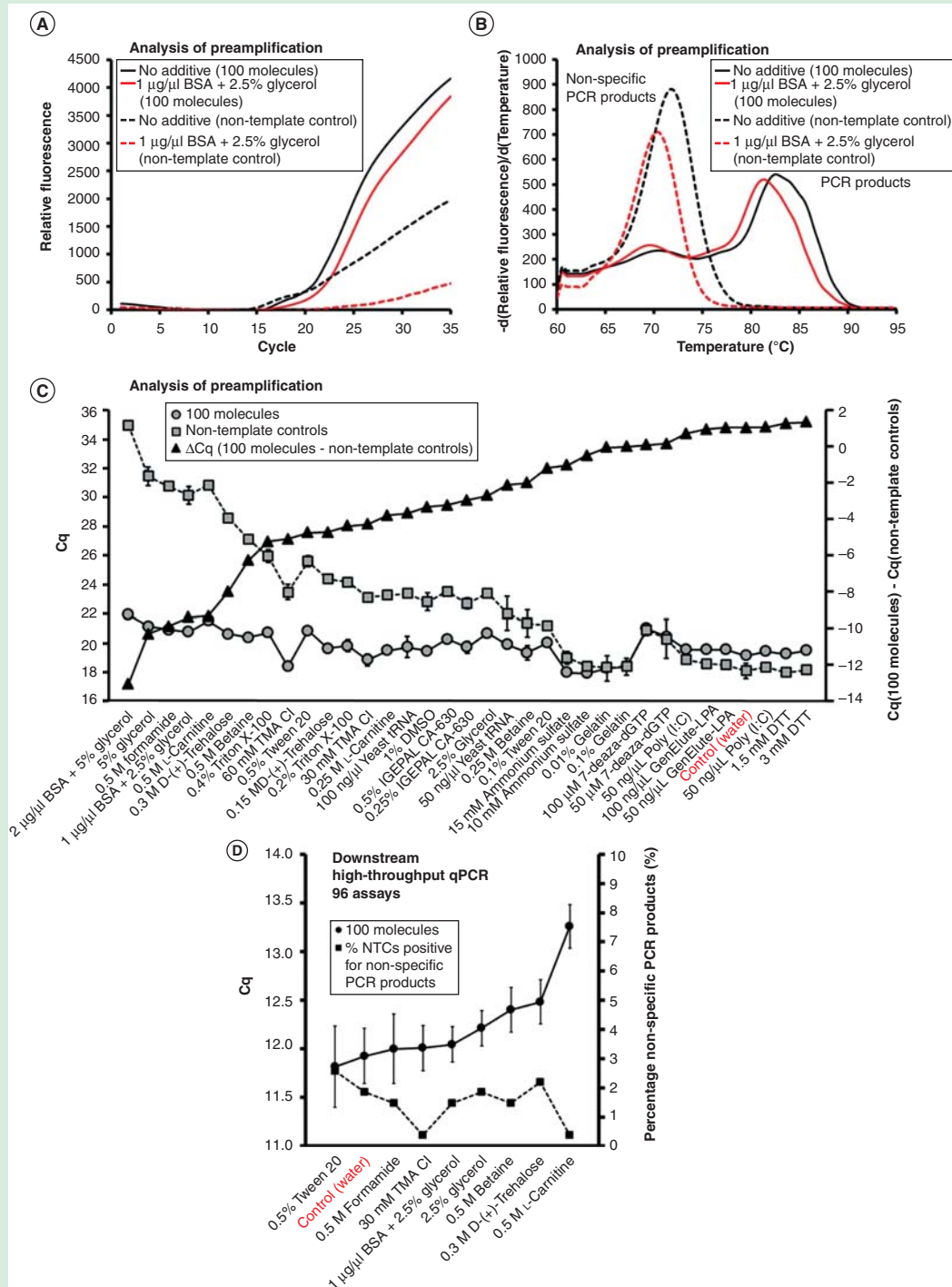


Figure 7. The effect of additives on preamplification specificity and efficiency. The yield and specificity of preamplification were evaluated at 35 conditions using 18 different additives. Analysis of preamplification: **(A, B)** preamplification response curves and corresponding melting curves for reactions in the presence of 1- $\mu\text{g}/\mu\text{l}$ bovine serum albumin with 2.5% glycerol or water. **(C)** Average $\text{C}_q \pm \text{SD}$ for positive ($n = 3$) and negative samples ($n = 3$) applying different conditions for preamplification. ΔC_q refers to the difference in C_q -values between positive and negative samples for each condition. Conditions are sorted according to ΔC_q -value. **(F)** High-throughput qPCR data of individual assays for nine selected conditions. Average $\text{C}_q \pm \text{SD}$ ($n = 3$) is shown. The right y-axis indicates the percentage of negative controls positive for nonspecific PCR product formation, calculated from the 91 assays performing accurately in the preamplification ($n_{\text{total}} = 273$, 3 negative qPCR controls per assay). 7-deaza-dGTP: 7-deaza-2'-deoxyguanosine 5'-triphosphate lithium salt; BSA: Bovine serum albumin; DMSO: Dimethyl sulfoxide; DTT: Dithiothreitol; LPA: GenElute-LPA; NTC: Non-template control; Poly(I:C): Polyinosinic-polycytidylic acid potassium salt; TMA Cl: Tetramethylammonium chloride.

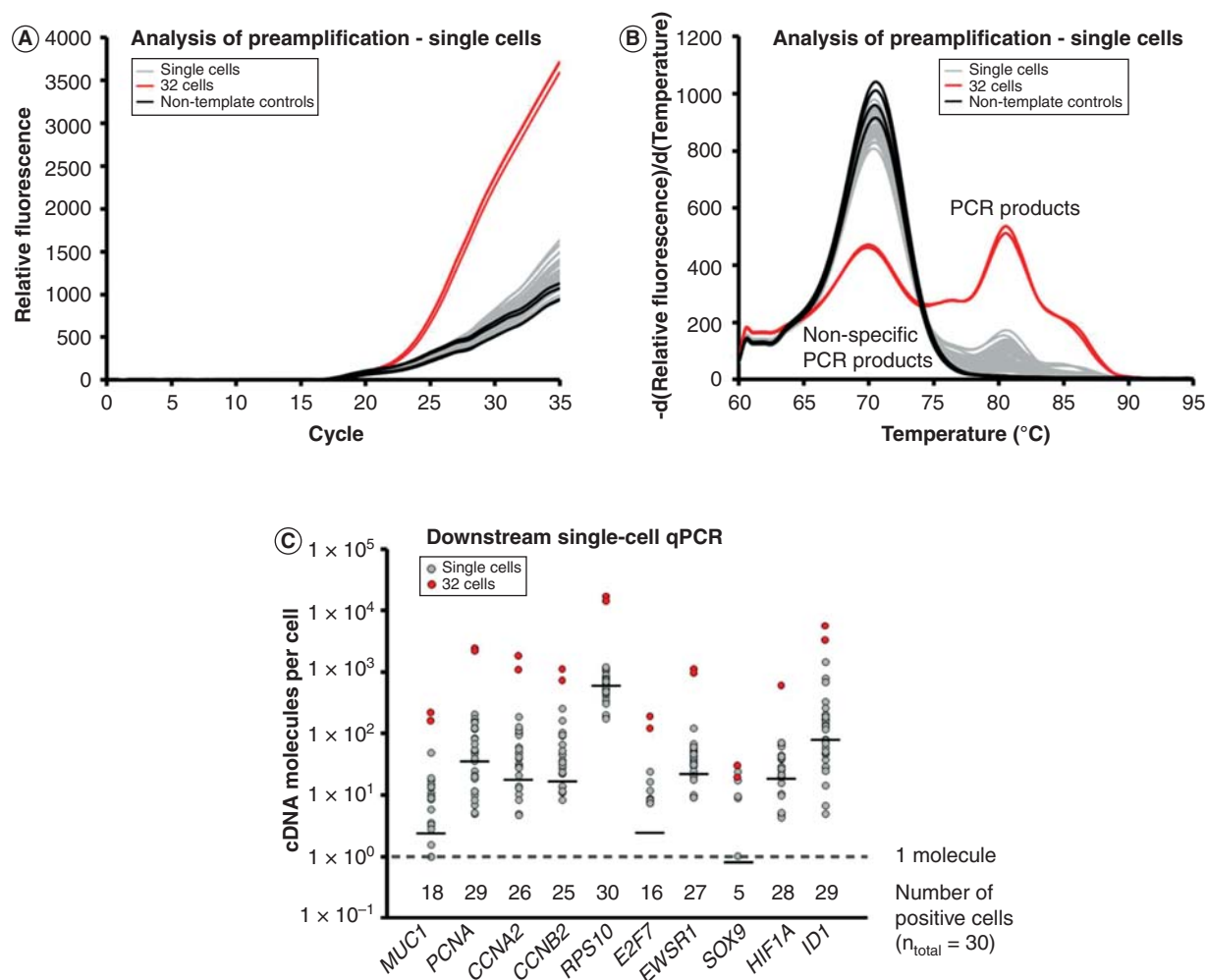


Figure 8. Single-cell analysis. Gene expression profiling of 30 individual MCF-7 cells using targeted preamplification. Analysis of preamplification: **(A)** preamplification curves and corresponding **(B)** melting curves for reactions in the presence of $1 \mu\text{g}/\mu\text{l}$ bovine serum albumin and 2.5% glycerol. **(C)** Dot plots displaying the expression pattern of 10 selected genes.

conducted for 20 cycles [11]. Yet, for samples with higher initial template concentrations fewer cycles should be applied to avoid exiting the exponential phase. Parameters, comprising the dNTP concentration, reaction volume and template concentration, determine the number of preamplification cycles that can be performed and still keep the reaction within its dynamic range. Our experimental data (FIGURE 2) showed that up to $\sim 10^6$ initial target molecules in total could be accurately preamplified for 20 cycles. In practice, when setting up preamplification for samples of unknown target concentrations, one may initially analyze a few selected, ubiquitously expressed transcripts, such as *GAPDH* or *ACTB*, by regular qPCR and based on these data design the pre-amplification protocol. As presented here, it is also possible to validate the preamplification protocol using a nonspecific reporter such as SYBR Green I and test for appearance of the preamplification response curve and specific product formation by melting curve analysis.

Analysis of highly multiplexed preamplification revealed that large quantities of nonspecific PCR products were formed. This was due to the high total primer concentration and the presence of numerous different primers. Counter-intuitively, the overall performance of individual assays in downstream qPCR analysis improves with increasing number of assays included in the preamplification. This may be explained by the fact that nonspecific PCR products formed during preamplification will only interfere with the downstream singleplex PCR if the particular nonspecific PCR product is complementary to the two primers used in the singleplex PCR. Hence, the larger the number of primers used in the preamplification the larger is the number of possible primer-to-primer interactions that may occur, increasing the amount of aberrant PCR products. However, the probability that the downstream singleplex qPCR is contaminated by carryover of a nonspecific PCR product that is complementary to the primers of that

particular qPCR assay decreases as the total number of primers increases.

Primer concentration, temperature and duration of the annealing step are dependent factors in preamplification. To reduce nonspecific PCR product formation in multiplex PCR, the primer concentrations are reduced tenfold for the preamplification compared to normal singleplex PCR. To maintain high preamplification efficiency applying low primer concentration, the annealing time is extended, usually to 3 min or longer. The rationale for this is that primers at lower concentrations need more time to locate to their specific target sequences. All primers applied in this study were designed to have a melting temperature around 60°C. As expected, the preamplification performed best using a similar annealing temperature.

In an attempt to reduce nonspecific PCR product formation, we evaluated the effects of several PCR additives that may improve enzymatic reactions involving nucleic acids (TABLE 2). Several of the additives reduced the formation of nonspecific PCR products in preamplification, but did not improve the performance of the individual assays. Most likely, this is because our assays were extensively optimized for high efficiency, specificity and sensitivity. For less optimized assays, or in the context of next-generation sequencing where extensive formation of nonspecific PCR products may steal sequencing capacity and reduce the amount of informative reads, additives such as bovine serum albumin in combination with glycerol or formamide may improve performance.

On the basis of our findings presented here, we provide the following recommendations for accurate targeted preamplification:

- The number of preamplification cycles should be sufficient to produce at least five (accurate sensitivity), but preferably

35 (accurate precision), molecules per aliquot used in downstream qPCR.

- A few highly abundant targets will not affect the preamplification performance of other assays.
- It is advantageous to use a large assay pool in preamplification.
- A final individual primer concentration of about 40 nM.
- Primer annealing at 60°C for 3 min or longer.

Acknowledgements

The authors are grateful to S Dolatabadi for primer design and to S Busch for scientific discussion of data.

Financial & competing interests disclosure

A Ståhlberg is supported by the Assar Gabrielssons Research Foundation, LUA/ALF Västra Götaland, Johan Jansson Foundation for Cancer Research, Swedish Cancer Society, Swedish Society for Medical Research, Swedish Research Council, Swedish Society for Medicine, BioCARE National Strategic Research Program at University of Gothenburg, VINNOVA, Wilhelm and Martina Lundgren Foundation for Scientific Research and Åke Winbergs Foundation. A Ståhlberg is a shareholder of the TATAA Biocenter. M Kubista is supported by grants ERDF (LK21305 and BIOCEV CZ.1.05/1.1.00/02.0109), Ministry of Youth, Education and Sports of the Czech Republic (AV0Z50520701). M Kubista is a shareholder and employee of the TATAA Biocenter and MultiD Analyses. G Landberg is supported by the Swedish Research Council, BioCARE National Strategic Research Program at University of Gothenburg, VINNOVA and Swedish Cancer Society. D Svec is supported by the Academy of Science, Czech Republic. D Svec is a shareholder of the TATAA Biocenter. The authors have no other relevant affiliations or financial involvement with any organization or entity with a financial interest in or financial conflict with the subject matter or materials discussed in the manuscript apart from those disclosed.

Key issues

- Analyses of limited sample sizes, including rare tissues, liquid biopsies, fine-needle aspirates and single cells are becoming important in numerous research and clinical assessments.
- Quantification of small numbers of DNA and RNA molecules usually requires preamplification for accurate analysis by downstream qPCR or next-generation sequencing.
- The most common strategy for targeted preamplification is based on multiplex PCR using pools of specific primer pairs, but the properties of the reaction are poorly understood.
- The overall performance of target preamplification can be studied in real-time, using SYBR Green I detection chemistry followed by melting curve analysis.
- The applied number of preamplification cycles should be sufficient to produce at least five (accurate sensitivity), but preferably 35 (accurate precision), molecules per aliquot used in downstream qPCR.
- The amount of initial template molecules, number of assays used, primer concentration, annealing time and annealing temperature are key parameters that influence the sensitivity, specificity, efficiency and reproducibility of targeted preamplification.
- Addition of additives, including bovine serum albumin in combination with glycerol or formamide, may improve preamplification by reducing the formation of nonspecific PCR products.
- Single-cell gene expression profiling is feasible using qPCR, applying carefully optimized targeted preamplification.
- On the basis of experimental data, we are able to provide guidelines how to perform accurate targeted preamplification for downstream applications.

References

Papers of special note have been highlighted as:

• of interest

•• of considerable interest

1. Dalerba P, Kalisky T, Sahoo D, et al. Single-cell dissection of transcriptional heterogeneity in human colon tumors. *Nat Biotechnol* 2011;29(12):1120-7
2. Guo G, Huss M, Tong GQ, et al. Resolution of cell fate decisions revealed by single-cell gene expression analysis from zygote to blastocyst. *Dev Cell* 2010;18(4):675-85
3. Norrman K, Strombeck A, Semb H, Stahlberg A. Distinct gene expression signatures in human embryonic stem cells differentiated towards definitive endoderm at single-cell level. *Methods* 2012;59(1):59-70
4. Patel AP, Tirosh I, Trombetta JJ, et al. Single-cell RNA-seq highlights intratumoral heterogeneity in primary glioblastoma. *Science* 2014;344(6190):1396-401
5. Bengtsson M, Stahlberg A, Rorsman P, Kubista M. Gene expression profiling in single cells from the pancreatic islets of Langerhans reveals lognormal distribution of mRNA levels. *Genome Res* 2005;15(10):1388-92
- **Single-cell study revealing that transcript levels have lognormal expression features in mammalian cells.**
6. Raj A, van Oudenaarden A. Nature, nurture, or chance: stochastic gene expression and its consequences. *Cell* 2008;135(2):216-26
7. Brady G, Barbara M, Iscove NN. Representative in Vitro cDNA Amplification From Individual Hemopoietic Cells and Colonies. *Methods Mol Cell Biol* 1990;2:17-25
8. Eberwine J, Yeh H, Miyashiro K, et al. Analysis of gene expression in single live neurons. *Proc Natl Acad Sci USA* 1992;89(7):3010-14
9. Lao K, Xu NL, Sun YA, et al. Real time PCR profiling of 330 human micro-RNAs. *Biotechnol J* 2007;2(1):33-5
10. Lao K, Xu NL, Yeung V, et al. Multiplexing RT-PCR for the detection of multiple miRNA species in small samples. *Biochem Biophys Res Commun* 2006;343(1):85-9
11. Livak KJ, Wills QF, Tipping AJ, et al. Methods for qPCR gene expression profiling applied to 1440 lymphoblastoid single cells. *Methods* 2012;59(1):71-9
- **Detailed methodology study, describing single-cell gene expression profiling using high-throughput qPCR.**
12. Rusnakova V, Honsa P, Dzamba D, et al. Heterogeneity of astrocytes: from development to injury - single cell gene expression. *PLoS One* 2013;8(8):e69734
13. Tang F, Hajkova P, Barton SC, et al. MicroRNA expression profiling of single whole embryonic stem cells. *Nucleic Acids Res* 2006;34(2):e9
- **First multiplex PCR based preamplification protocol for miRNA expression profiling.**
14. Stahlberg A, Kubista M. The workflow of single-cell expression profiling using quantitative real-time PCR. *Expert Rev Mol Diagn* 2014;14(3):323-31
15. Kojima Y, Acar A, Eaton EN, et al. Autocrine TGF-beta and stromal cell-derived factor-1 (SDF-1) signaling drives the evolution of tumor-promoting mammary stromal myofibroblasts. *Proc Natl Acad Sci USA* 2010;107(46):20009-14
16. Stahlberg A, Bengtsson M, Hemberg M, Semb H. Quantitative transcription factor analysis of undifferentiated single human embryonic stem cells. *Clin Chem* 2009;55(12):2162-70
17. Stahlberg A, Thomsen C, Ruff D, Aman P. Quantitative PCR analysis of DNA, RNAs, and proteins in the same single cell. *Clin Chem* 2012;58(12):1682-91
18. Ye J, Coulouris G, Zaretskaya I, et al. Primer-BLAST: a tool to design target-specific primers for polymerase chain reaction. *BMC Bioinformatics* 2012;13:134
19. Kubista M, Andrade JM, Bengtsson M, et al. The real-time polymerase chain reaction. *Mol Aspects Med* 2006;27(2-3):95-125
20. Stahlberg A, Andersson D, Aurelius J, et al. Defining cell populations with single-cell gene expression profiling: correlations and identification of astrocyte subpopulations. *Nucleic Acids Res* 2011;39(4):e24
21. Bustin SA, Benes V, Garson JA, et al. The MIQE guidelines: minimum information for publication of quantitative real-time PCR experiments. *Clin Chem* 2009;55(4):611-22
22. Stahlberg A, Rusnakova V, Forootan A, et al. RT-qPCR work-flow for single-cell data analysis. *Methods* 2013;59(1):80-8
23. SciencePrimer.com. Available from: <http://scienceprimer.com/copy-number-calculator-for-realtime-pcr>
24. Stahlberg A, Kubista M, Aman P. Single-cell gene-expression profiling and its potential diagnostic applications. *Expert Rev Mol Diagn* 2011;11(7):735-40
25. Bettgowda C, Sausen M, Leary RJ, et al. Detection of circulating tumor DNA in early- and late-stage human malignancies. *Sci Transl Med* 2014;6(224):224ra224
- **First comprehensive study showing that circulating cell-free tumor DNA can be accurately quantified in multiple tumor entities.**
26. Pantel K, Alix-Panabieres C. Real-time liquid biopsy in cancer patients: fact or fiction? *Cancer Res* 2013;73(21):6384-8
27. Alix-Panabieres C, Pantel K. Challenges in circulating tumour cell research. *Nat Rev Cancer* 2014;14(9):623-31
28. Motz M, Paabo S, Kilger C. Improved cycle sequencing of GC-rich templates by a combination of nucleotide analogs. *Biotechniques* 2000;29(2):268-70
29. Musso M, Boccardi R, Parodi S, et al. Betaine, dimethyl sulfoxide, and 7-deaza-dGTP, a powerful mixture for amplification of GC-rich DNA sequences. *J Mol Diagnost* 2006;8(5):544-50
30. Olive DM, Simsek M, Al-Mufti S. Polymerase chain reaction assay for detection of human cytomegalovirus. *J Clin Microbiol* 1989;27(6):1238-42
31. Henke W, Herdel K, Jung K, et al. Betaine improves the PCR amplification of GC-rich DNA sequences. *Nucleic Acids Res* 1997;25(19):3957-8
32. Kang J, Lee MS, Gorenstein DG. The enhancement of PCR amplification of a random sequence DNA library by DMSO and betaine: application to in vitro combinatorial selection of aptamers. *J Biochem Biophys Methods* 2005;64(2):147-51
33. Giambernardi TA, Rodeck U, Klebe RJ. Bovine serum albumin reverses inhibition of RT-PCR by melanin. *Biotechniques* 1998;25(4):564-6
34. Nagai M, Yoshida A, Sato N. Additive effects of bovine serum albumin, dithiothreitol, and glycerol on PCR. *Biochem Mol Biol Int* 1998;44(1):157-63
35. Svec D, Andersson D, Pekny M, et al. Direct cell lysis for single-cell gene expression profiling. *Front Oncol* 2013;3:274

36. Spiess AN, Mueller N, Ivell R. Trehalose is a potent PCR enhancer: lowering of DNA melting temperature and thermal stabilization of taq polymerase by the disaccharide trehalose. *Clin Chem* 2004; 50(7):1256-9
37. Zhang Z, Kermekchiev MB, Barnes WM. Direct DNA amplification from crude clinical samples using a PCR enhancer cocktail and novel mutants of Taq. *J Mol Diagnost* 2010;12(2):152-61
38. Bookstein R, Lai CC, To H, Lee WH. PCR-based detection of a polymorphic BamHI site in intron 1 of the human retinoblastoma (RB) gene. *Nucleic Acids Res* 1990;18(6):1666
39. Sarkar G, Kapelner S, Sommer SS. Formamide can dramatically improve the specificity of PCR. *Nucleic Acids Res* 1990; 18(24):7465
40. Ohler LD, Rose EA. Optimization of long-distance PCR using a transposon-based model system. *PCR Methods Appl* 1992; 2(1):51-9
41. Sachdeva R, Simm M. Application of linear polyacrylamide coprecipitation of denatured templates for PCR amplification of ultra-rapidly reannealing DNA. *Biotechniques* 2011;50(4):217-19
42. Cheng S, Fockler C, Barnes WM, Higuchi R. Effective amplification of long targets from cloned inserts and human genomic DNA. *Proc Natl Acad Sci USA* 1994;91(12):5695-9
43. Fortier ME, Kent S, Ashdown H, et al. The viral mimic, polyinosinic:polycytidylic acid, induces fever in rats via an interleukin-1-dependent mechanism. *Am J Physiol* 2004;287(4):R759-66
44. Chevet E, Lemaitre G, Katinka MD. Low concentrations of tetramethylammonium chloride increase yield and specificity of PCR. *Nucleic Acids Res* 1995;23(16): 3343-4
45. Kovarova M, Draber P. New specificity and yield enhancer of polymerase chain reactions. *Nucleic Acids Res* 2000;28(13): E70
46. Melchior WB Jr, Von Hippel PH. Alteration of the relative stability of dA-dT and dG-dC base pairs in DNA. *Proc Natl Acad Sci USA* 1973;70(2):298-302
47. George S, Sokolenko S, Aucoin MG. Rapid and cost-effective baculovirus sample preparation method as a viable alternative to conventional preparation for quantitative real-time PCR. *J Virol Methods* 2012;182;1-2:27-36
48. Peper G, Fankhauser A, Merlin T, et al. Direct real-time quantitative PCR for measurement of host-cell residual DNA in therapeutic proteins. *J Pharmaceut Biomed Anal* 2014;100:123-30
49. Wang QT, Xiao W, Mindrinos M, Davis RW. Yeast tRNA as carrier in the isolation of microscale RNA for global amplification and expression profiling. *BioTechniques* 2002; 33(4):788, 790, 792 passim